THE ASTROPHYSICAL JOURNAL, 451:575–584, 1995 October 1

OSSE OBSERVATIONS OF BLAZARS

K. MCNARON-BROWN,[1] W. N. JOHNSON, G. V. JUNG,[2] R. L. KINZER, J. D. KURFESS,
M. S. STRICKMAN, AND C. D. DERMER
E. O. Hulburt Center for Space Research, Code 7650, Naval Research Laboratory, Washington, DC 20375
D. A. GRABELSKY, W. R. PURCELL, AND M. P. ULMER
Department of Physics and Astronomy, Northwestern University, Evanston, IL 60208
M. KAFATOS AND P. A. BECKER
CSI, George Mason University, Fairfax, VA 22030
AND
R. STAUBERT AND M. MAISACK
Astronomisches Institut der Universität Tübingen, 72076 Tübingen, Germany
Received 1995 February 8; accepted 1995 April 4

ABSTRACT

Results are reported on observations obtained with the Oriented Scintillation Spectrometer Experiment (OSSE) instrument on the *Compton Gamma Ray Observatory* (*CGRO*) of 17 active galactic nuclei (AGNs) known to exhibit blazar properties at other wavelengths. These observations span the period from 1991 June through 1994 May. Of the 33 high-confidence EGRET detections of blazars during *CGRO* observing phases 1 and 2 (1991 May 16–1993 September 7), OSSE has observed eight and detected five, namely 3C 273, 3C 279, PKS 0528+134, CTA 102, and 3C 454.3. Additionally, OSSE has detected the BL Lac sources H1517+65.6 and PKS 2155−304, which were not detected with EGRET. Variability in the energy band 50–150 keV is observed for all of the detected AGNs. The OSSE blazar sources are all well described by simple power-law models with photon number indices, Γ, varying from 1.0 to 2.1 among sources. When combined with available, although not necessarily contemporaneous, COMPTEL and EGRET observations, four to five detected blazars show clear evidence for spectral breaks between the hard X-ray and medium-energy gamma-ray bands. The exception is the combined OSSE/EGRET data for 3C 279 during 1991 October, where a simple power law with $\Gamma \approx 1.9$ works equally well. Gamma-ray evidence for beaming in CTA 102, PKS 0528+134, and 3C 454.3 is presented.

Subject headings: BL Lacertae objects: general — galaxies: active — gamma rays: observations — X-rays: galaxies

1. INTRODUCTION

The discovery of a large number of active galactic nuclei (AGNs) emitting >100 MeV gamma rays by the EGRET instrument on the *Compton Gamma Ray Observatory* (*CGRO*) has stimulated considerable interest in the high-energy and multifrequency behavior of these objects. Before the launch of *CGRO*, some AGNs were known to emit in the hard X-ray and soft gamma-ray ($\gtrsim$0.1 MeV) range (see, e.g., Rothschild et al. 1983; Bassani & Dean 1983), but the only quasar detected at photon energies $E \gg 1$ MeV was the nearby quasar 3C 273. Although this source was not detected at soft gamma-ray energies, it was detected at $E > 50$ MeV with the *COS B* experiment (Swanenburg et al. 1978). The EGRET team has now reported 25 high-confidence detections of AGNs at $E > 100$ MeV in *CGRO* observing phase 1 (Fichtel et al. 1994) and eight more high-confidence detections of AGNs in phase 2 (von Montigny et al. 1995). These AGNs are all associated with compact, flat spectrum radio sources which are often found to exhibit superluminal motion, rapid optical variability, and high optical polarization. These sources differ from Seyfert AGNs at hard X-ray energies by displaying a broader range of spectral indices (Williams et al. 1992; Sambruna et al. 1994). This class of objects, which includes BL Lac objects and highly polarized and optically violently variable (OVV) quasars, is generally referred to as the blazar class.

Blazars are thought to be AGNs with jets that are nearly aligned along the line of sight to the observer. The spectra of bright blazars generally have two broad maxima. Between radio and optical frequencies, blazars exhibit broad νF_ν spectral peaks occurring between $\approx 10^{11}$ and 10^{14} Hz (e.g., Impey 1987). This emission is usually attributed to Doppler-boosted synchrotron radiation emitted by nonthermal electrons in a relativistically outflowing plasma. The new high-energy observations demonstrate the presence of a second broad spectral peak at gamma-ray energies. Nearly simultaneous observations show that the gamma-ray emission of 3C 279 dominates its bolometric luminosity (Maraschi et al. 1994); on the basis of noncontemporaneous observations (von Montigny et al. 1995), this is apparently the case for several quasars as well. The OSSE observations are important to the study of blazars because they help establish the energy of the peak of the νF_ν spectra and the magnitudes of the spectral breaks from the hard X-ray and medium-energy gamma-ray regimes. Unlike arguments for gamma-ray transparency in the EGRET energy range (Mattox et al. 1993; Maraschi, Ghisellini, & Celotti 1992), gamma-ray transparency arguments based on observations in the soft gamma-ray regime require no additional assumptions about the source location of the soft photons.

[1] Also CSI, George Mason University.
[2] Also Universities Space Research Association.

In this paper we report on OSSE observations of 17 blazars and give spectral results on seven of these sources detected during the period from 1991 June to 1994 May. The blazars detected are 3C 273, 3C 279, CTA 102, PKS 0528+134, 3C 454.3, H1517+65.6, and PKS 2155−304; the first five have also been detected with EGRET. In § 2 we describe the observations, present results of temporal and spectral analyses of the data, and describe the multiwavelength character of the blazars detected with OSSE. In § 3 the implications of the observations on models of blazars are considered. We present our conclusions in § 4.

2. OBSERVATIONS AND ANALYSIS

2.1. *Instrument Description and Blazar Observations*

The Oriented Scintillation Spectrometer Experiment, one of four instruments on *CGRO*, is designed to detect gamma rays in the 0.05–10 MeV range. OSSE comprises four independent phoswich spectrometers of identical design that are each actively shielded and passively collimated. Tungsten collimators define a $3.^{\circ}8 \times 11.^{\circ}4$ full width at half-maximum (FWHM) gamma-ray aperture.

OSSE observations consist of a sequence of 2 minute observations of a source field alternated with 2 minute offset-pointed background measurements. The 2 minute duration is selected to be short relative to the typical orbital background variations. When possible, source-free field offsets $4.^{\circ}5$ on either side of the source position along the detector scan plane are used for background observations. Different background field configurations are used when required to avoid fields confused with likely gamma-ray sources. Quadratic interpolation in time among the measured background intervals is used to estimate the background during the source observation. The background estimtes are then subtracted from the associated source accumulations to form 2 minute difference spectra. These spectra are further screened for environmental effects and transient phenomena. Screened 2 minute spectra are then summed into daily average spectra and finally into spectra averaged over the entire observation interval. A more detailed description of OSSE, its performance, and spectral data analysis procedures can be found in Johnson et al. (1993).

In the period 1991 June through 1994 May, OSSE observed six BL Lac sources and 11 QSOs in 45 separate observations. Observations made in support of *CGRO* Guest Investigations are not presented here. The characteristics of the observed blazars are summarized in Table 1. Marks in the EGRET or OSSE columns of the table indicate positive detection by that instrument in one or more observations.

Unlike the other instruments on *CGRO*, OSSE's small field of view requires the selection of specific targets for observation. Generally, two sources are selected for each observation interval—one in the field of view of COMPTEL and EGRET, and the other approximately 90° away so that it may be observed when the first source is occulted by the Earth. Thus, it is possible for OSSE to observe targets without simultaneous observation from COMPTEL and EGRET.

The OSSE targets are selected when the *CGRO* observation timeline is being developed, well before the observation. Consequently, during the first year of the *CGRO* mission, most of the OSSE AGN targets were selected based on historical X-ray and gamma-ray measurements. OSSE observations of the EGRET-discovered gamma-ray–emitting blazars could not be scheduled until the later phases of the mission. Since OSSE's 192° of motion permit viewing of targets outside the field of view of COMPTEL and EGRET, the constraints on the *CGRO* viewing timeline occasionally required scheduling of OSSE blazar targets at orientations which did not permit simultaneous COMPTEL/EGRET observations. Table 2 summarizes the OSSE blazar observations and indicates those observation intervals which provided simultaneous coverage with COMPTEL/EGRET. Also provided are the detected fluxes from the sources in the 0.05–0.15 MeV, 0.15–0.5 MeV, and 0.5–1.0 MeV energy bands. Upper limits are specified at the 95% confidence level or 2 σ. As indicated in the table, most objects were observed during more than one viewing period (VP). In such cases, the first entry for the source is the weighted average of all the observations. The last column in the table indicates the total live time of high-quality data on the source in detector-seconds. As seen in Table 2, four sources are detected at a significance of 5 σ or greater; they are, in order of decreasing significance, 3C 273, 3C 279, PKS 0528+134, and PKS 2155−304. Three additional sources are detected at a significance of 3 σ or greater: CTA 102, H1517+65.6, and 3C 454.3. OSSE has only upper limits for 4C 15.05, Mrk 421, and QSO 0716+714, three sources positively detected with EGRET. A more detailed discussion of the results for 3C 273 is presented elsewhere (Johnson et al. 1995).

Only OSSE data from those blazar observations with positive detections (here defined as >3 σ) have been used in this analysis. For PKS 0528+134, however, the first two observations were very short and consequently produced detections or upper limits with lower significance but which were consistent with the same flux found in the longer viewing period. The spectra from all three observations of PKS 0528+134 were therefore summed together to produce an average spectrum. Omitting the short observing periods from the analysis did not produce statistically different results.

2.2. *Temporal Analysis*

The time dependences of the integral photon fluxes in the 0.05–0.15 MeV range are shown in Figure 1 for the OSSE blazars 3C 273, 3C 279, PKS 0528+134, and CTA 102, respectively. The data within each viewing period for each source have been averaged into 3 to 4 day intervals. Searches for variability in sources detected with weak (3–5 σ) significance, such as PKS 2155−304, were not improved by subdividing data into smaller viewing periods and therefore are not displayed in the figure. Variability can be seen in all of the sources shown in Figure 1, although statistically significant (>2 σ) variability for 3C 279, CTA 102, 3C 454.3, and PKS 2155−304 is found only by comparing the average fluxes between different viewing periods (see Table 2).

Flux variations for 3C 273 from VP 3 to VP 8 indicate variation by as much as a factor of 3 on timescales of ≈ 2 months, and day-to-day variations as large as 25% are seen for VP 3 alone, suggesting source variability over the 2 week period at >2.5 σ significance (Johnson et al. 1995). Variability by a factor of ~ 2 is observed for 3C 279 over the period of a year (i.e., between VPs 10 and 39, 91/263–92/251). The 3 day flux averages of PKS 0528+134 in the 1994 May observation are only weakly consistent with a constant flux (χ^2 probability $\sim 5 \times 10^{-2}$). CTA 102 observations are also inconsistent with a constant flux (χ^2 probability $\sim 6 \times 10^{-3}$) over a period of 2 months (i.e., between VPs 317 and 323). Interperiod variability was found for PKS 2155−304 and 3C 454.3 as well.

1995ApJ...451..575M

TABLE 1

CHARACTERISTICS OF BLAZARS OBSERVED WITH OSSE

			CHARACTERISTICS								
SOURCE	EGRET	OSSE	OVV	BL Lac	Superluminal[a]	$F_{5\,\mathrm{GHz}}$ (Jy)	Spectral Index[b]	Radio Reference	Optical Polarization	Optical Reference	z
0202+149 (4C 15.05)	X				...	[2.37, 2.55]	-0.38 ± 0.05	1	4.0%	5	...
0219+428 (3C 66A)				X	...	[3.72, 3.81]	-0.86 ± 0.09	1	2.2	4	0.444
0438−436.....					...	[6.23, 7.81]	$+0.27 \pm 0.06$	1	4.7	5	2.852
0528+134 (PKS).....	X	X	X		5.9	3.98 ± 0.14	$+0.47 \pm 0.19$	1	0.3	5	2.06
0548−322 (PKS).....				X	...	0.084	0.35	2	2.7	2	0.069
0716+714.....	X			X	?	1.12 ± 0.01	$+0.21 \pm 0.06$	1	...		...
0736+017.....					...	[1.88, 2.26]	-0.26 ± 0.11	1	8.4	5	0.191
0834−201.....					...	[3.52, 3.93]	-0.18 ± 0.09	1	1.0	5	2.752
1028+313.....					...	0.66	...	3	0.25	6	0.177
1101+384 (Mrk 421)	X			X	[1.8, 2.5]	0.530	...	4	<0.2	4	0.031
1226+023 (3C 273)	X	X	X		[5.8, 10.7]	[34.90, 44.59]	-0.01 ± 0.07	1	2.5	5	0.158
1253−055 (3C 279)	X	X	X		[2.9, 12.2]	[13.39, 16.58]	$+0.31 \pm 0.06$	1	19.0	5	0.536
1517+656.....		X		X	...	...	...		...		...
2155−304 (PKS).....		X		X	...	0.341	0.37	2	1.3	2	0.117
2201+044 (4C 04.77)				X	...	...	...		...		0.028
2230+114 (CTA 102).....	X	X			[0.0, 24]	[3.63, 3.78]	-0.50 ± 0.05	1	10.9	5	1.037
2251+158 (3C 454.3)	X	X	X		[−1.5, 11.8]	[9.01, 24.00]	$+0.50 \pm 0.06$	1	16.0	5	0.859

[a] Range of apparent superluminal velocities from Vermeulen & Cohen 1994, Impey 1987, & Pohl et al. 1995. $H_0 = 75\,h$ km s^{-1} Mpc^{-1}.

[b] Two point spectral index as determined between 2700 MHz and 5000 MHz.

REFERENCES.—(1) Kühr et al. 1981; (2) Stocke et al. 1985; (3) Shastri et al. 1993; (4) Ulvestad et al. 1983; (5) Impey & Tapia 1990; (6) Wills et al. 1992.

TABLE 2

OSSE BLAZAR OBSERVATIONS

Source[a]	Viewing Period	Date Interval[b]	Flux[c] (0.05–0.15 MeV)	Flux[c] (0.15–0.5 MeV)	Flux[c] (0.5–1.0 MeV)	Observation Time[d]
3C 273	...	...	10.63 ± 0.29	1.64 ± 0.09	0.29 ± 0.09	22.32
	3[e]	91/167–91/179	17.34 ± 0.48	2.54 ± 0.16	0.75 ± 0.15	8.13
	8	91/235–91/248	5.67 ± 0.76	0.91 ± 0.24	<0.46	3.76
	11[e]	91/277–91/290	3.58 ± 0.55	0.65 ± 0.17	<0.32	5.74
	36.5	92/226–92/228	15.68 ± 2.23	1.22 ± 0.73	1.55 ± 0.66	0.27
	39	92/252–92/256	18.35 ± 1.37	2.61 ± 0.44	0.44 ± 0.41	0.79
	204[e]	92/358–92/364	8.70 ± 1.56	1.03 ± 0.49	<0.90	0.71
	205[e]	92/364–93/005	7.03 ± 1.76	1.68 ± 0.54	<1.00	0.66
	206[e]	93/005–93/012	10.00 ± 1.92	<1.16	<1.05	0.52
	303.4	93/274–93/290	19.68 ± 1.31	2.33 ± 0.38	<0.72	0.91
3C 279	...	...	3.30 ± 0.50	0.43 ± 0.15	0.22 ± 0.14	6.64
	10	91/263–91/276	6.22 ± 0.65	0.87 ± 0.20	<0.38	3.21
	39	92/246–92/251	<2.41	<0.80	<0.73	0.88
	204[e]	92/358–92/364	<3.23	<0.96	<0.89	0.74
	205[e]	92/364–93/005	<3.67	<1.12	<1.03	0.61
	206[e]	93/005–93/012	<3.78	0.74 ± 0.57	<1.04	0.47
3C 454.3	...	...	<1.19	<0.36	<0.33	6.77
	317	94/048–94/060	4.46 ± 1.20	0.47 ± 0.37	0.46 ± 0.34	2.44
	319	94/060–94/067	<2.93	<0.88	<0.83	1.21
	319.5	94/074–94/081	<2.53	<0.72	<0.67	1.68
	323	94/081–94/090	<2.18	<0.66	<0.61	1.44
4C 04.77	37	92/234–92/240	<4.70	<1.58	<1.47	0.31
4C 15.05	324	94/109–94/116	<8.74	<2.60	<2.36	0.16
CTA 102	...	...	1.00 ± 0.52	0.44 ± 0.16	0.35 ± 0.15	5.93
	316	94/023–94/032	<2.02	<0.62	<0.57	1.74
	317	94/048–94/060	<1.56	0.41 ± 0.24	0.44 ± 0.23	2.37
	323	94/081–94/095	3.98 ± 0.95	0.87 ± 0.29	0.64 ± 0.28	1.82
H1517+65.6.....	212	93/068–93/082	4.88 ± 1.26	<0.76	<0.70	1.00
Mrk 421	...	...	<0.91	<0.30	<0.26	5.64
	5	91/194–91/206	<1.63	<0.52	<0.49	1.86
	6	91/207–91/220	<1.27	0.34 ± 0.22	<0.42	2.49
	9.5	91/256–91/262	<2.03	<0.68	<0.63	1.11
	232	93/236–93/238	<5.62	1.42 ± 0.83	1.45 ± 0.80	0.18
PKS 0528+134	...	...	4.16 ± 0.49	0.82 ± 0.15	0.18 ± 0.14	8.71
	41	92/283–92/289	3.52 ± 2.23	<1.34	<1.20	0.67
	44	92/309–92/322	2.03 ± 1.63	1.37 ± 0.50	<0.90	1.28
	322	94/095–94/109	4.46 ± 0.53	0.78 ± 0.17	0.16 ± 0.15	7.09
PKS 0548−322.....	31	92/164–92/177	2.60 ± 2.06	<1.24	<1.16	0.42
PKS 2155−304	...	...	0.87 ± 0.62	<0.38	<0.35	4.44
	42[e]	92/289–92/303	4.86 ± 0.96	0.45 ± 0.29	<0.54	1.50
	319	94/060–94/067	<2.40	<0.74	0.58 ± 0.35	1.27
	319.5	94/074–94/081	<2.08	<0.64	<0.58	1.68
QSO 0219+428.....	323	94/081–94/095	<2.22	<0.70	<0.66	1.53
QSO 0438−436.....	325	94/116–94/130	<2.02	<0.60	<0.55	2.58
QSO 0716+714.....	...	...	<1.21	<0.42	<0.33	4.15
	230	93/208–93/215	<1.86	<0.96	<0.58	1.31
	319[e]	94/060–94/067	<1.59	<0.48	<0.44	2.84
QSO 0736+016.....	3	91/168–91/179	<1.36	<0.46	<0.45	2.62
QSO 0834−201.....	...	...	<2.16	<0.68	<0.64	1.52
	41	92/283–92/289	<4.52	<1.38	<1.29	0.36
	44	92/309–92/322	<2.47	<0.78	0.38 ± 0.37	1.16
QSO 1028+313.....	...	...	<1.13	<0.40	<0.38	5.71
	301	93/230–93/236	<3.01	<0.88	0.56 ± 0.41	0.63
	322[2]	94/095–94/109	<1.54	<0.46	<0.42	3.16
	326[e]	94/130–94/137	1.63 ± 1.00	<0.59	<0.54	1.92

[a] First line for each source is average of all observations.
[b] Year/day of year.
[c] Units: 10^{-3} photons cm^2 s^{-1} MeV^{-1}; upper limits are 2 σ.
[d] Units: 10^5 detector-seconds.
[e] Contemporaneous observations with COMPTEL/EGRET.

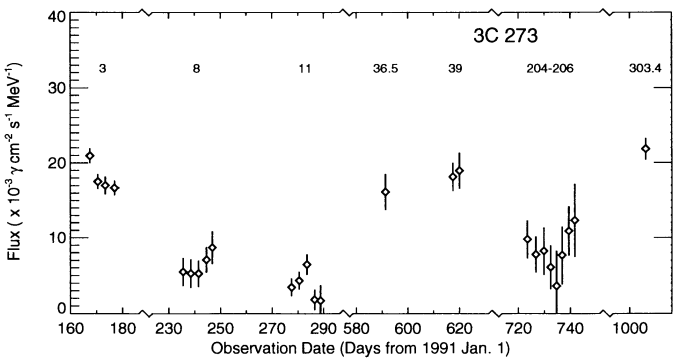

FIG. 1*a*

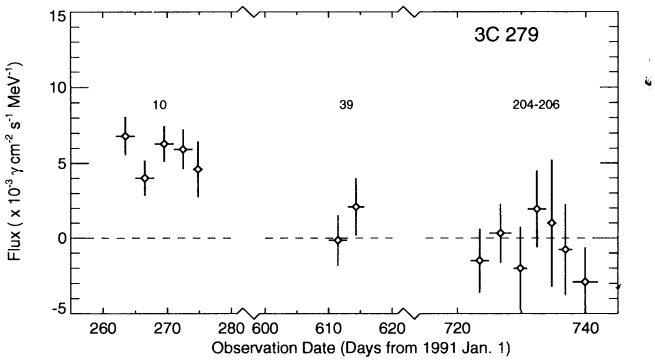

FIG. 1*b*

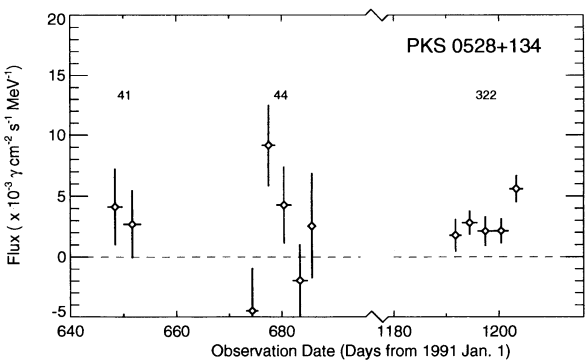

FIG. 1*c*

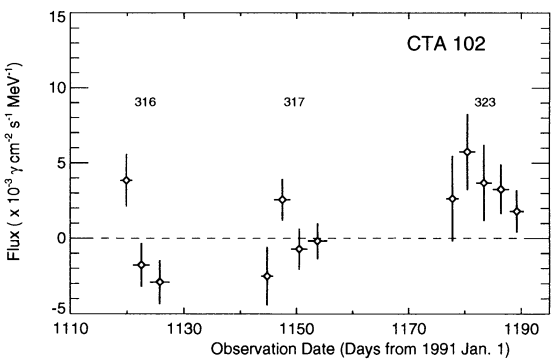

FIG. 1*d*

FIG. 1.—Time-averaged flux in the 50–150 keV band from (*a*) 3C 273, (*b*) 3C 279, (*c*) PKS 0528+134, and (*d*) CTA 102 observed with OSSE. Each data point represents the average flux for a contiguous 3–4 day period. *CGRO* viewing period numbers are displayed above the data points. Negative fluxes are due to background estimation uncertainties and are not statistically significant.

2.3. *Spectral Analysis*

The spectral fitting procedure consists of folding model photon spectra through the OSSE response matrix and adjusting the model parameters to minimize, through a χ^2 test, the deviations between the model count spectrum and the observed count spectrum. Using the OSSE data alone, the spectra are reasonably well described by single power-law models, $N(E)\,dE = F_0(E/E_0)^{-\Gamma}\,dE$, as indicated in Table 3. The uncertainties in this table are 68% confidence limits ($\Delta\chi^2 = 2.28$). The last column represents the statistical probability of observing a χ^2 value larger than the measured value, if the model truly represents the data.

When OSSE data are combined with the COMPTEL and EGRET measurements, there is evidence for significant softening in the spectra, particularly between the OSSE and EGRET energy bands. We have modeled these softenings of the spectra as broken power laws and have fitted the combined OSSE, COMPTEL, and EGRET data for five sources. For 3C 279, where we compare OSSE data for VP 10 and EGRET data (Kniffen et al. 1993) for VP 11, either a simple power-law model

TABLE 3

SPECTRAL FITS TO OSSE OBSERVATIONS USING SINGLE POWER-LAW MODEL

Source	*CGRO* Observation Dates[a]	Flux[b] at 100 keV	Power-Law Index[c]	χ^2/dof	χ^2 Probability
3C 273	91/167–91/179	$13.5^{+0.5}_{-0.5}$	$1.7^{+0.1}_{-0.1}$	20.5/23	0.61
3C 279	91/263–91/276	$4.6^{+0.6}_{-0.6}$	$2.1^{+0.4}_{-0.4}$	6.2/6	0.40
3C 454.3	94/048–94/060	$4.1^{+1.2}_{-1.2}$	$1.5^{+0.6}_{-0.4}$	6.3/4	0.17
CTA 102	94/081–94/095	$2.8^{+1.0}_{-1.1}$	$1.0^{+0.7}_{-0.6}$	9.1/6	0.17
H1517+656	93/068–93/080	$3.6^{+1.2}_{-1.2}$	$1.9^{+1.0}_{-0.8}$	3.2/5	0.67
PKS 0528+134.....	92/283–94/109	$2.7^{+0.5}_{-0.5}$	$1.2^{+0.3}_{-0.3}$	5.2/5	0.39
PKS 2155−304.....	92/298–92/303	$3.8^{+0.9}_{-0.9}$	$1.8^{+0.6}_{-0.4}$	3.3/5	0.66

[a] Year/day of year.
[b] Units: 10^{-3} photons cm^{-2} s^{-1} MeV^{-1}.
[c] Differential photon number index.

TABLE 4

POWER LAW WITH BREAK FOR OSSE, COMPTEL, AND EGRET FITS

Source	E_{Break}(MeV)	Γ_{lower}	$\Delta\Gamma$	χ^2/dof	χ^2 Probability
3C 273	$1.0^{+0.9}_{-0.4}$	$1.7^{+0.1}_{-0.1}$	$0.7^{+0.1}_{-0.1}$	27.6/28	0.49
3C 279	$3.6^{+4000.}_{-3.5}$	$1.8^{+0.2}_{-1.2}$	$0.3^{+0.3}_{-0.3}$	11.6/14	0.64
3C 279[a]	...	$1.93^{-0.02}_{-0.02}$	...	14.6/16	0.55
3C 454.3	$10.0^{+75.0}_{-9.1}$	$1.7^{+0.2}_{-0.2}$	$0.5^{+0.4}_{-0.3}$	12.1/9	0.21
CTA 102	$2.3^{+20.0}_{-1.5}$	$1.0^{+0.7}_{-0.6}$	$1.7^{+0.7}_{-0.7}$	11.7/14	0.63
PKS 0528+134	$17.0^{+33.0}_{-10.0}$	$1.5^{+0.2}_{-0.1}$	$1.1^{+0.2}_{-0.3}$	11.5/14	0.65

NOTE.—Only data from 3C 273 are contemporaneous among the instruments.
[a] Single power-law fit.

with $\Gamma = 1.93 \pm 0.02$ or a broken power-law are acceptable over the entire fit range. The best fits are tabulated in Table 4 and displayed in Figure 2. Model uncertainties are determined by the 68% confidence interval for joint variation of four interesting parameters ($\Delta\chi^2 = 4.70$). It is important to recognize that most of the data sets represent noncontemporaneous observations; only for the VP 3 observation of 3C 273 are there contemporaneous OSSE, COMPTEL, and EGRET data. Source variations between the epoch of the OSSE observation and that of the COMPTEL and EGRET measurements could affect both the energy of the power-law break and the magnitude of the break. However, these observations clearly indicate that the emitted power of these blazars is strongly peaked at MeV energies. Large $\Delta\Gamma$ ($\Delta\Gamma > 0.5$) is found in four of these five sources, the most extreme being CTA 102, where $\Delta\Gamma = 1.7 \pm 0.7$.

Two of the six sources listed in Table 3, PKS 2155−304 and H1517+65.6, have not been positively detected with EGRET. Figure 3 shows the derived OSSE spectra and best-fit power-law models for these sources with the corresponding 2 σ upper limits from EGRET (Fichtel et al. 1994). The OSSE/EGRET data for PKS 2155−304 are contemporaneous (VP 42), but the data for H1517+65.6 are not (OSSE data are from VP 212, and EGRET data are from VP 22). Clearly, a break in the spectrum is required in both sources between 200 keV and 100 MeV. For the remaining three EGRET blazars observed with OSSE (4C 15.05, Mrk 421, and QSO 0716+714), only upper limits were obtained. These upper limits are not in conflict with extrapolations of their EGRET spectra into the OSSE energy range (see Fichtel et al. 1994).

2.4. *X-Ray and Gamma-Ray Properties of Detected Blazars*

EGRET first reported detection of 3C 279 during VP 3 (Bertsch et al. 1991; Hartman et al. 1992); significant variation in the >100 MeV intensity was observed during a <2 day interval (Kanbach et al. 1992; Kniffen et al. 1993). The spectrum during VP 3 is well fitted by a single power law from >100 MeV to ~3 GeV with $\Gamma = 1.9$ (Fichtel et al. 1994). The gamma-ray emission decreased after the flare but was still detectable when observed with OSSE during VP 10 and with EGRET during VP 11. The >100 MeV flux dropped by a factor of >6 in VP 11 from its peak in VP 3; the spectrum was found to soften to $\Gamma \cong 2.1$ in independent fits made to OSSE and EGRET data. Combined data from OSSE and EGRET during VPs 10 and 11, respectively, are consistent with a single power-law with index $\Gamma \approx 1.9$, as given in Table 3.

The quasar CTA 102 was observed 4 times with the EGRET instrument with a photon spectrum well represented by a power law with $\Gamma = 2.6 \pm 0.2$ (Nolan et al. 1993), one of the softest blazars observed with EGRET. The only published report of X-rays from CTA 102 was the detection with the *Einstein Observatory* (Zamorani et al. 1981; Worrall et al. 1987) at a flux level of 0.4 μJy near 1 keV. OSSE observed CTA 102 in three viewing periods, with only VP323 providing a positive detection at the 4 σ level. The blazar 3C 454.3 is separated from CTA 102 by ~8° and was alternately observed with CTA 102 during VPs 317 and 323. Care was taken so that the two were well isolated in the OSSE scan direction during these observations. Fitting OSSE data alone reveals a hard power-law spectrum with $\Gamma \approx 1.0$. Fits to the combined noncontemporaneous COMPTEL and EGRET data with OSSE show the greatest break in the spectral index of all the sources reported here ($\Delta\Gamma \approx 1.7$).

There is not much prior high-energy information on H1517+65.6. It was detected with *Einstein* (Elvis et al. 1992), but little spectral information was obtained. Fits to OSSE data reveal a spectrum with $\Gamma \sim 1.9$.

PKS 0528+134 was first detected at gamma-ray energies (>100 MeV) with EGRET (Kanbach et al. 1992) during two *CGRO* observations toward the Galactic anticenter at the beginning of the mission (1991 April and May). The high-energy spectral index in the 100 MeV–1 GeV range was reported to be 2.6 ± 0.1 (Hunter et al. 1993). This quasar exhibits variability of its >100 MeV emission on a timescale $\lesssim$2 days and is a COMPTEL source (Schönfelder 1994). The power-law fit to the average OSSE spectrum for PKS 0528+134 shows a hard index of $\Gamma = 1.2 \pm 0.3$. Fitting the OSSE data with noncontemporaneous EGRET data shows a break in the spectrum around $E \sim 17$ MeV with $\Delta\Gamma \approx 1.1$. It is important to note that there is a 3 yr gap between the OSSE and COMPTEL/EGRET data and that the EGRET data used in this analysis are not from any of the reported flares of this source in the >100 MeV energy range (von Montigny et al. 1995).

PKS 2155−304 is one of the most intensively studied AGNs. It is well known for its short timescales of variability at optical to X-ray wavelengths. It was first discovered as an X-ray source with the *HEAO 1* satellite (Schwartz et al. 1979; Griffiths et al. 1979). The X-ray luminosity typically ranges over a factor of 10, with a factor of 4 increase in 4 hr reported on one occasion from *EXOSAT* observations (Morini et al. 1986). The source also exhibited a high degree of variability during observations with the *Ginga* satellite, with a dynamic

range of a factor of 7 in the 2–6 keV band among five different observations (Sembay et al. 1993). It has a steep hard X-ray spectrum with photon index typically in the range $1.5 \lesssim \Gamma \lesssim 2.5$ (e.g., Urry, Mushotzky, & Holt 1986). Spectral fits to the 1989 October 2 *Ginga* data reveal a photon index of $\Gamma = 1.60 \pm 0.01$ above 4 keV (Sembay et al. 1993). NGC 7172, a potentially confusing source in the Seyfert 2 class ($\sim 1.^{\circ}8$ from PKS 2155−304), is contained in the OSSE source field of VP 42. The other periods (VP 319 and VP 319.5) were designed to isolate the contributions of NGC 7172 and PKS 2155−304. Unfortunately, neither target was detectable during these observations.

High-energy gamma radiation was observed from the OVV quasar 3C 454.3 with EGRET during VP 19 (92/023–92/037). Its high-energy emission showed a power-law photon spectrum with $\Gamma = 2.2 \pm 0.1$ (Hartman et al. 1993). The flux density (>100 MeV) was observed to vary within the range $(0.4–1.4) \times 10^{-6}$ photon cm^{-2} s^{-1} on a timescale of less than 1 week. The *Ginga* observations of 3C 454.3 show its spectrum to be softer than those seen from most other OVV X-ray spectra (Ohashi et al. 1989). The power-law fit to the OSSE spectrum alone reveals an index with $\Gamma \approx 1.5$.

3. DISCUSSION

We now consider the implications of the OSSE observations on the standard model for blazars (e.g., Blandford & Rees 1978; Blandford & Königl 1979). In this model, jet emission is produced by plasma that is ejected at relativistic speeds from an accreting supermassive black hole. The OSSE observations address the question of beaming in two ways: through the Elliot-Shapiro (1974) relation, modified to the gamma-ray regime (Dermer & Gehrels 1995), and through gamma-ray transparency arguments (e.g., Stecker & Tsuruta 1972; Maraschi et al. 1992; Blandford 1993; Mattox et al. 1993; Dermer & Gehrels 1995), also modified to the OSSE energy range.

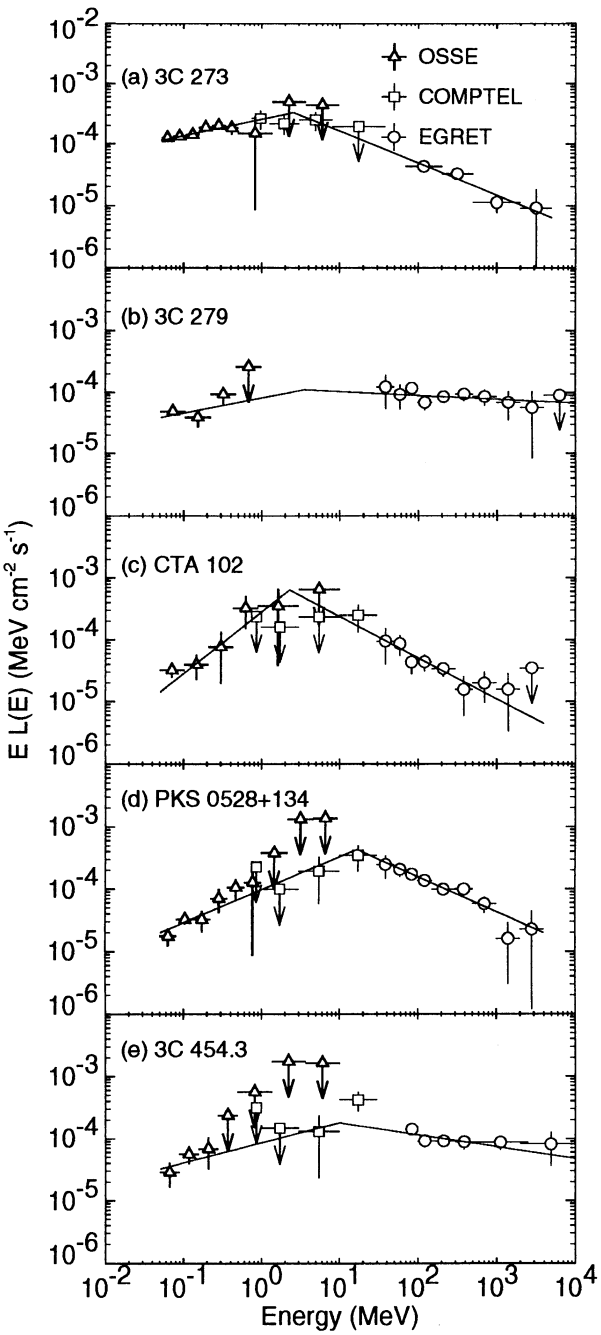

FIG. 2.—Compton *GRO* spectrum of five blazars are displayed as $E^2 \times$ differential photon flux. The solid line indicates the best fit to each of the data as a broken power law. Only the COMPTEL and EGRET data for 3C 273 are contemporaneous with OSSE data. (*a*) COMPTEL data from Williams et al. (1995); EGRET data from von Montigny et al. (1993) and Fichtel et al. (1994) (*b*) EGRET data from Kniffen et al. (1993). (*c*) COMPTEL data from Blom et al. (1995); EGRET data from Nolan et al. (1993). (*d*) COMPTEL data from Collmar et al. (1994); EGRET data from Hunter et al. (1993). (*e*) COMPTEL data from Blom et al. (1995); EGRET data from Hartman et al. (1993).

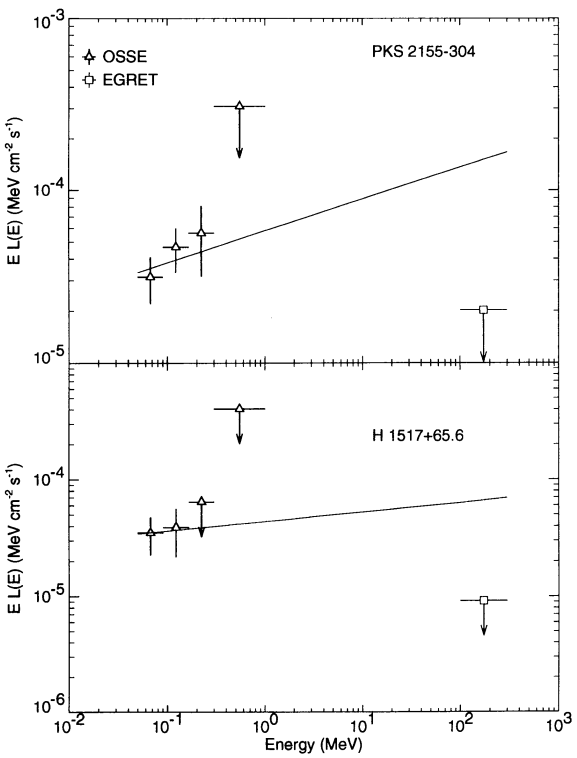

FIG. 3.—Deconvolved photon spectra measured for PKS 2155−304 and H1517+656, respectively, are displayed as $E^2 \times$ differential photon flux with their best-fit power-law models. EGRET data for both sources are from Fichtel et al. (1994).

3.1. *Luminosity and Mass Estimates*

The Elliot-Shapiro relation tests for beaming by noting that a lower limit to the mass is derived from the inferred isotropic luminosity, assuming Eddington-limited accretion. If the source accretes below the Eddington limit, then even larger black hole masses are implied. An upper limit to the mass is inferred from the emission size scale implied by the variability timescale using light-travel time arguments, since the size scale must be larger than a few Schwarzschild radii. If the two mass limits conflict, beaming is implied.

We first calculate the minimum black hole masses implied by the OSSE observations, assuming that the radiation is isotropically emitted and produced by Eddington-limited accretion onto a supermassive black hole. Denoting the observed photon flux by $\Phi(\epsilon)$ [photons cm^{-2} s^{-1} ϵ^{-1}], where the dimensionless photon energy $\epsilon = h\nu/m_e c^2$, the luminosity produced by a source at redshift z over an energy band ϵ_l to ϵ_u is given by

$$L[(1+z)\epsilon_l, (1+z)\epsilon_u] \approx \frac{4\pi d_L^2 (m_e c^2)}{(1+z)^2} \int_{\epsilon_l}^{\epsilon_u} d\epsilon\, \epsilon \Phi\left(\frac{\epsilon}{1+z}\right). \quad (1)$$

The luminosity distance $d_L = 2cf(z)/H_0$, where $f(z) = 1 + z - (1+z)^{1/2}$, appropriate to a $q_0 = \frac{1}{2}$ cosmology. The luminosities inferred from the OSSE observations of blazars are given in Table 5. The inferred isotropic luminosities in the OSSE energy range, redshifted back to the cosmological frame, are in the range $\sim 10^{45}$–10^{49} ergs s^{-1}. The inferred value of 4.6×10^{48} ergs s^{-1} measured for PKS 0528+134 would represent the most luminous quiescently radiating source known, assuming that the photons are isotropically emitted, which is probably not correct as we show below. The blazar luminosities extend, of course, to much lower values. For example, the OSSE upper limit for Mrk 421 implies that its inferred isotropic luminosity is $\sim 10^{44}$ ergs s^{-1}.

The implied minimum black hole mass for Eddington-limited accretion in the Thomson regime is given by $M_8 \lesssim L_T/(1.26 \times 10^{46}$ ergs s$^{-1})$, where L_T is the total luminosity for emission in the Thomson regime, $\epsilon \ll 1$. Using the Klein-Nishina cross section, from which the factor $\kappa(\epsilon)$ can be derived (given by Pozdnyakov, Sobol, & Sunyaev 1983; Dermer & Gehrels 1995), the radiation force exerted through Compton scattering from a point source of isotropic emission with spectral luminosity $L(\epsilon)$ is given by

$$\boldsymbol{F}_C = \frac{\sigma_T \hat{r}}{4\pi r^2 c} \int_0^\infty d\epsilon\, L(\epsilon)\kappa(\epsilon). \quad (2)$$

Eddington-limited accretion for a hydrogen plasma implies that $|\boldsymbol{F}_G| = -GMm_H \hat{r}/r^2 > |\boldsymbol{F}_C|$. We obtain an expression for the minimum mass of a black hole which is assumed to emit isotropic radiation by steady, Eddington-limited accretion, in units of $10^8\ M_\odot$, given by

$$M_8^C \lesssim \frac{4\pi d_L^2 (m_e c^2)(1+z)^{-2}}{1.26 \times 10^{46}} \int_{\epsilon_l(1+z)}^{\epsilon_u(1+z)} d\epsilon\, \Phi\left(\frac{\epsilon}{1+z}\right) \epsilon\, \kappa(\epsilon). \quad (3)$$

The implied minimum black hole masses are listed in Table 5 for the OSSE blazars, under the assumptions of isotropic radiation and Eddington-limited accretion. The measurement of PKS 0528+134 implies the largest black hole mass, namely $M \gtrsim 7 \times 10^9\ M_\odot$. The inferred black hole masses for CTA 102 and 3C 454.3 are also $\gtrsim 10^9\ M_\odot$, and the black hole masses are $\gtrsim 10^7$–$10^8\ M_\odot$ for the other three sources. Using light-travel time arguments and assuming a spherical geometry with radius R, the minimum size scale of the emission site is $R \lesssim c\,\delta t_{obs}/(1+z)$, where δt_{obs} is the measured variability timescale. Because R must be greater than the Schwarzschild radius $R_S = 2GM/c^2 = 3.0 \times 10^{13} M_8$ cm, δt_{obs} implies a maximum black hole mass. For PKS 0528+134, the maximum mass implied from the variability timescale is nearly equal to the minimum mass implied from the Eddington-limited argument. If further observations show a statistically significant conflict between the two implied mass determinations, then the assumption of isotropic emission would be called into question.[3] The other OSSE blazars listed in Table 5 are less luminous or variable, so the Elliot-Shapiro relation also does not imply beaming for them.

3.2. *Gamma-Ray Transparency*

Gamma-ray transparency arguments (Mattox et al. 1993; Maraschi et al. 1992; Blandford 1993) provide an independent test for beaming. These arguments proceed as follows: Assume that the source is at rest in the cosmological frame so that the observed gamma-ray variability timescale δt_{obs} implies a maximum emission-region size scale $R \lesssim c\delta t_{obs}/(1+z)$, from simple light-travel time arguments. If X-rays observed from blazars are produced in the same region as gamma rays, then the pair production optical depth $\tau_{\gamma\gamma}$ for gamma rays above

[3] A 2 week observation of PKS 0528+134 with OSSE, COMPTEL, and EGRET was performed during VP 413 (1995 March 7–1995 March 21); however, analysis has not been completed.

TABLE 5

PAIR PRODUCTION OPTICAL DEPTHS AND BLACK HOLE MASS LIMITS OF GAMMA-RAY AGNs

Source	δt_{obs}(days)	z	ϵ_l, ϵ_u[a]	Luminosity[b]	$M_{8,min}$[c]	$M_{8,max}$[d]	$\tau_{\gamma\gamma}(E = 1$ MeV)
3C 273	3	0.158	[0.1, 2.0]	4.3	1.5	220	1.1
3C 279	334	0.540	[0.1, 1.8]	14	4.7	1.9×10^4	7.2×10^{-2}
3C 454.3	12	0.859	[0.1, 3.9]	90	14	560	13
CTA 102	21	1.037	[0.1, 2.8]	170	25	890	13
PKS 0528+134.....	3	2.06	[0.1, 2.4]	460	70	85	250
PKS 2155−304.....	853	0.117	[0.1, 3.3]	0.73	0.21	6.6×10^4	3.9×10^{-4}

[a] $\epsilon \equiv E/mc^2$.
[b] 10^{46} ergs s^{-1}, $h = 1$.
[c] Derived assuming Eddington-limited accretion with the isotropic luminosity.
[d] Based on variability observations.

100 MeV greatly exceeds unity for 1633+382 (Mattox et al. 1993), 3C 279 (Maraschi et al. 1992), and PKS 0528+134, so that beaming is implied. Beaming is not required if one considers only the photon attenuation of gamma rays in the EGRET energy range that interact with other gamma rays (Dermer & Gehrels 1995). Becker & Kafatos (1995) show that gamma rays do not need to be produced at large distances from the central source if X-rays are assumed to be produced in an accretion disk and that the angle-dependent $\gamma\gamma$ opacity provides intrinsic collimation of gamma rays.

Here we derive the pair production optical depth of photons in the OSSE energy range interacting with other photons in this range, so that no additional assumptions are necessary. From the formulation of Gould & Schréder (1967), we can write

$$\tau_{\gamma\gamma}(\epsilon_1) \cong R \int_{2/\epsilon_1}^{\infty} d\epsilon\, \sigma_{\gamma\gamma}(s) n_{\rm ph}(\epsilon)\,, \tag{4}$$

where

$$n_{\rm ph}(\epsilon)d\epsilon \cong \frac{d_L^2}{R^2 c} \frac{\Phi[\epsilon/(1+z)]}{(1+z)^2}\, d\epsilon \tag{5}$$

is the differential number of photons per unit volume with ϵ between ϵ and $\epsilon + d\epsilon$ (see eq. [1]). The invariant quantity $s = 2\epsilon\epsilon_1$, and the pair-production cross section $\sigma_{\gamma\gamma}(s)$ is quoted in Gould & Schréder (1967). Substituting equation (5) into equation (4), we obtain

$$\tau_{\gamma\gamma}(\epsilon_1) \cong \frac{d_L^2}{c^2 \delta t_{\rm obs}} \int_{\max[2/\epsilon_1(1+z)^2,\, \epsilon_l]}^{\epsilon_u} d\epsilon\, \sigma_{\gamma\gamma}(s)\Phi(\epsilon)\,, \tag{6}$$

where $\Phi(\epsilon)$ is the measured OSSE photon flux in dimensionless units, and ϵ_l and ϵ_u are the smallest and largest photon energies measured from a given source with OSSE (see Table 5). Here we have assumed that photons are emitted from a homogeneous spherical region with size scale $R \lesssim c\delta t_{\rm obs}/(1+z)$.

Equation (6) is integrated using the best-fit power-law parameters for the OSSE blazars given in Table 3. Table 5 lists values of the pair production optical depth for photons of energy 1 MeV at the present epoch. As shown in Figures 2 and 3, all blazars except 3C 279 and PKS 2155−304 were observed by OSSE at energies above 1 MeV. We see from Table 5 that CTA 102, PKS 0528+134, and 3C 454.3 have $\tau_{\gamma\gamma}(1\ {\rm MeV}) \gg 1$ and that the largest pair production opacity is $\approx$250 for PKS 0528+134. Thus, the intrinsic spectrum of photons near $E \approx (1+z)$ MeV would be attenuated by orders of magnitude if the gamma rays were produced isotropically in a stationary source. The gamma-ray transparency constraints can be weakened if a nonspherical geometry is considered or if the $\lesssim$500 keV and $\gtrsim$500 keV emission sites are at separate locations, but the smoothness of the OSSE gamma-ray spectra does not suggest the existence of two distinct spectral components. Hence, the detection of gamma rays up to 1 MeV in PKS 0528+134, CTA 102, and 3C 454.3 provides evidence in favor of beaming.

3.3. *Constraints on Models from Spectral Observations*

Values of $\Delta\Gamma > 0.5$ are measured in combined noncontemporaneous OSSE/EGRET observations of four gamma-ray blazars, as seen from Table 4. Spectral breaks significantly greater than 0.5 are in conflict with the simplest versions of one-component, time-integrated Compton cooling jet models (Dermer & Schlickeiser 1993; Sikora, Begelman, & Rees 1993) which predict that $\Delta\Gamma = 0.5$. Compton models with the injection of monoenergetic rather than power-law electrons (e.g., Melia & Königl 1989; Protheroe, Mastichiadis, & Dermer 1992) can produce spectral index changes >0.5 but cannot produce an X-ray spectrum harder than $\Gamma = 1.5$. Power-law fits to the data from CTA 102, PKS 0528+134, and 3C 454.3 (see Table 4), however, do show $\Gamma < 1.5$. Cascades initiated by photomeson production from high-energy protons (Mannheim & Biermann 1992) may fit the spectral data but do not produce rapidly variable emission because of the relatively small proton energy loss rates. Spectral breaks >0.5 are also produced in hot accretion disk models (e.g., Becker & Kafatos 1994) because of incomplete cooling by pion decay electrons and positrons, but require extremely massive ($\sim 10^{10}\ M_\odot$) black holes.

4. CONCLUSIONS

Observations with *CGRO* show that gamma-ray blazars constitute an extraordinarily luminous class of quiescently radiating sources. We find that the luminosities of gamma-ray blazars in the OSSE energy range between 50 keV and 1 MeV extend to $\approx 5 \times 10^{48}$ ergs s^{-1}, assuming that the gamma rays are isotropically emitted. Of the 25 blazars detected at high confidence with EGRET during Phase 1 (Fichtel et al. 1994), OSSE has observed eight and detected five. Comparison of the fluxes and spectral indices measured in the OSSE and EGRET energy ranges implies that the spectra of these sources soften between the two energy ranges. Spectral softening between low- and medium-energy gamma rays is also suggested by the comparison of the relatively few COMPTEL detections of blazars compared with the number detected with EGRET (Schönfelder 1994). The noncontemporaneous spectra shown in Figure 2 illustrate this behavior, which appears to be a generic feature of gamma-ray blazars.

Of the five EGRET blazars detected with OSSE, four show clear evidence of spectral softening in the 1–15 MeV energy range when fitted with noncontemporaneous COMPTEL and EGRET data. The exception to this is 3C 279 during 1991 October, in which a simple power-law model with $\Gamma = 1.93 \pm 0.02$ works as well as a broken power-law model. The spectral breaks, $\Delta\Gamma$, in these four cases range from 0.5 to 1.7, the most extreme being CTA 102. These results provide strong constraints on external scattering blazar models. OSSE has detected two additional blazars that have not been reported as EGRET sources. Extrapolation to high energies of the spectral fits to PKS 2155−304 and H1517+65.6 also implies spectral softening between the OSSE and EGRET energy ranges (see Fig. 3).

The blazar PKS 0528+134 is the brightest quiescently radiating source known, if one assumes that the high-energy radiation is isotropically emitted. Gamma-ray emission from CTA 102, PKS 0528+134, and 3C 454.3 would be severely attenuated at 1 MeV photon energies if the emitting regions are stationary, so that either relativistic outflow or anisotropic gamma-ray emission is implied for these sources. OSSE gamma-ray observations presently provide the strongest evidence for beaming from gamma-ray data alone and are in accord with the scenario that blazar radiation is anisotropically emitted from relativistically outflowing jets.

Note added in manuscript.—PKS 2155−304 has been recently detected by EGRET (Vestrand, Stacy, & Sreekumar 1995).

We thank B. McBreen for providing the PKS 2155−304 data associated with the *CGRO* Guest Investigation Program. This work was supported under NASA grants DPR S-10987C, DPR S-30931-F, NAD 5-2025, and DARA 50 OR 92054.

REFERENCES

Bassani, L., & Dean, A. J. 1983, Space Sci. Rev., 35, 367
Becker, P. A., & Kafatos, M. 1994, in AIP Conf. Proc. 304, The Second Compton Symposium, ed. C. E. Fichtel, N. Gehrels, & J. P. Norris (New York: AIP), 620
———. 1995, ApJ, in press
Bertsch, D. L., et al. 1991, IAU Circ., No. 5311, 1
Blandford, R. D. 1993, in Compton Gamma Ray Observatory, ed. M. Friedlander, N. Gehrels, & D. J. Macomb (New York: AIP), 533
Blandford, R. D., & Königl, A. 1979, ApJ, 232, 34
Blandford, R. D., & Rees, M. J. 1978, in Pittsburgh Conference on BL Lac Objects, ed. A. M. Wolfe (Pittsburgh: Univ. Pittsburgh Press), 328
Blom, J. J., et al. 1995, A&A, in press
Collmar, W., et al. 1994, in AIP Conf. Proc. 304, The Second Compton Symposium, ed. C. E. Fichtel, N. Gehrels, & J. P. Norris (New York: AIP), 659
Dermer, C. D., & Gehrels, N. 1995, ApJ, 447, 103
Dermer, C. D., & Schlickeiser, R. 1993, ApJ, 416, 458
Elliot, J. L., & Shapiro, S. L. 1974, ApJ, 192, L3
Elvis, M., Plummer, D., Schachter, J., & Fabbiano, G. 1992, ApJS, 80, 257
Fichtel, C. E., et al. 1994, ApJS, 94, 551
Gould, R. J., & Schréder, G. P. 1967, Phys. Rev., 155, 1404
Griffiths, R. E., Tapia, S., Briel, U., & Chaisson, L. 1979, ApJ, 234, 810
Hartman, R. C., et al. 1992, ApJ, 385, L1
Hartman, R. C., et al. 1993, ApJ, L41
Hunter, S. D., et al. 1993, ApJ, 409, 134
Impey, C. 1987, in Superluminal Radio Sources, ed. J. A. Zensus & T. J. Pearson (Cambridge: Cambridge Univ. Press), 233
Impey, C., & Tapia, S. 1990, ApJ, 354, 124
Johnson, W. N., et al. 1993, ApJS, 86, 693
Johnson, W. N., et al. 1995, ApJ, 445, 182
Kanbach, G., et al. 1992, IAU Circ., No. 5431
Kniffen, D. A., et al. 1993, ApJ, 411, 133
Kühr, H., Witzel, A., Pauliny-Toth, I. I. K., & Nauber, U. 1981, A&AS, 45, 367
Mannheim, K., & Biermann, P. 1992, A&A, 253, L21
Maraschi, L., et al. 1994, ApJ, 435, L91
Maraschi, L., Ghisellini, G., & Celotti, A. 1992, ApJ, 397, L5
Mattox, J. R., et al. 1993, ApJ, 410, 609
Melia, F., & Königl, A. 1989, ApJ, 340, 162
Morini, M., Chiappetti, L., Maccagni, D., Maraschi, L., Molteni, D., Tanzi, E. G., Treves, A., & Wolter, A. 1986, ApJ, 306, L71
Nolan, P. L., et al. 1993, ApJ, 414, 453
Ohashi, T., et al. 1989, in Proc. 23d ESLAB Symp. on Two Topics in X-Ray Astronomy (ESA SP-296) (Nordwijk: ESA), 837
Pohl, M., et al. 1995, A&A, in press
Pozdnyakov, L. A., Sobol, J. M., & Sunyaev, R. A. 1983, ApJSS, 2, 189
Protheroe, R. J., Mastichiadis, A., & Dermer, C. D. 1992, Astroparticle Phys., 1, 113
Rothschild, R. E., Mushotzky, R. F., Baity, W. A., Gruber, D. E. Matteson, J. L., & Peterson, L. E. 1983, ApJ, 269, 423
Sambruna, R. M., Barr, P., Giommi, P., Maraschi, L., Tagliaferri, G., & Treves, A. 1994, ApJS, 95, 371
Schönfelder, V. 1994, ApJS, 92, 593
Schwartz, D. A., Doxsey, R. E., Griffiths, R. E., Johnston, M. D., & Schwartz, J. 1979, ApJ, 229, L53
Sembay, S., et al. 1993, 404, 112
Shastri, P., Wilkes, B. J., Elvis, M., & McDowell, J. 1993, 410, 29
Sikora, M., Begelman, M., & Rees, M. 1994, ApJ, 421, 153
Stecker, F. W., & Tsurata, S. 1972, Nature, 235, 8
Stocke, J. T., Liebert, J., Schmidt, G., Gioia, I. M., Maccacaro, T., Schild, R. E., Maccagni, D., & Arp, H. 1985, ApJ, 298, 619
Swanenburg, B. N., et al. 1978, Nature, 275, 298
Ulvestad, J. S., Johnston, K. J., & Weiler, K. W. 1983, ApJ, 266, 18
Urry, C. M., Mushotzky, R. F., & Holt, S. S. 1986, ApJ, 305, 369
Vermeulen, R. C., & Cohen, M. H. 1994, ApJ, 430, 467
Vestrand, W. T., Stacy, J. G., & Sreekumar, P. 1995, IAU Circ., 6169
von Montigny, C., et al. 1993, A&AS, 97, 101
von Montigny, C., et al. 1995, ApJ, 440, 525
Wills, B., Wills, D., Breger, M., Antonucci, R. R., & Barvainis, R. 1992, ApJ, 398, 454
Williams, O. R., et al. 1992, ApJ, 389, 157
Williams, O. R., et al. 1995, A&A, in press
Worrall, D. M., Giommi, P., Tananbaum, H., & Zamorani, G. 1987, ApJ, 313, 596
Zamorani, G., et al. 1981, ApJ, 245, 357